J Mater Sci: Mater Electron (2017) 28:12268–12272
DOI 10.1007/s10854-017-7043-y

Synthesis and magnetic properties of manganese–zinc ferrite nanoparticles obtained via a hydrothermal method

Xin Li[1] · Rui Sun[1] · Baoyuan Luo[1] · Aijun Zhang[1] · Ailin Xia[1] · Chuangui Jin[1]

Received: 30 March 2017 / Accepted: 28 April 2017 / Published online: 3 May 2017

Abstract Manganese–zinc (MnZn) ferrite nanoparticles were synthesized via a hydrothermal method, and their structural and magnetic properties were studied. It was found that a low Fe content and the hydrothermal temperature play crucial roles in the synthesis of single phase MnZn ferrites. The hydrothermal temperature also affects the topography and the magnetic properties markedly. The best soft magnetic properties of $M_s = 45.5$ emu/g and $H_c = 0.68$ kA/m were obtained for the specimen with a Fe deficiency of 7% in the starting materials and hydrothermally synthesized at 180 °C.

1 Introduction

As one of the most important soft-magnetic materials, spinel manganese–zinc (MnZn) ferrite is widely used as the core of power transformers and inductors due to their relatively high initial magnetic permeability, high saturation magnetization and low power loss [1]. Nanoparticles have some attractive performances, which promotes the extensive studies of many magnetic materials, in which including nanoscale MnZn ferrite [2, 3]. As a main chemical method to prepare nanomaterials, the sol–gel technique is currently often used to obtain MnZn nanoferrites, such as the studies from Peng [1], Lutsev [4], Ebrahimi [5], Choi [6] and so on. As is well-known, the nanoparticles obtained via a hydrothermal or solvothermal method are homogeneous and ultrafine. However, compared with the sol–gel method, the hydrothermal or solvothermal method is seldom used to synthesize MnZn ferrite possibly due to the difficulty of formation of single phase. Recently, Freire and Drofenik [7, 8] studied the superparamagnetic properties and the effect of solvent composition on the structural and magnetic properties of MnZn ferrite nanoparticles. Rozman [9] studied the sintering of nanosized MnZn ferrite powders. However, the synthesis of single-phase MnZn ferrite was not discussed in these reports. Recently, we have systematically studied the synthesis of MnZn nanoferrites obtained via a hydrothermal method, and studied the effects of hydrothermal temperatures and low Fe content in the starting materials on the phase formation and magnetic properties.

2 Experimental

2.1 Synthesis of MnZn nanoparticles

MnZn ferrites with a nominal composition $(Mn_{0.4}Zn_{0.6})Fe_2O_4$ were synthesized via a hydrothermal method. Analytically pure nitrates ($Mn(NO_3)_2$, $Fe(NO_3)_3$, $Zn(NO_3)_2$ and NaOH) were used as the starting materials without further treatment. According to our previous study in spinel NiZnCu ferrites [10], excess Zn^{2+} ions of 5% in the starting materials benefit the synthesis of single-phase MnZn ferrites for a wet chemical method due to the loss of Zn^{2+} ions during the process of chemical reaction. A deficiency of Fe^{3+} ions (*DF*, 6 or 7%) in the starting materials was set to study the synthesis of single-phase MnZn ferrite. First, all the nitrates for preparing 4 mmol MnZn ferrites were dissolved in the 60 ml distilled water, and 1.37 g NaOH was dissolved in 15 ml distilled water. The NaOH solution was dropped into the mixed nitrates solution until the

✉ Ailin Xia
alxia@126.com

[1] Anhui Key Laboratory of Metal Materials and Processing, School of Materials Science and Engineering, Anhui University of Technology, Maanshan 243032, China

pH value is 11, and was simultaneously stirred vigorously by a magnetic stirrer for 10 min. Then, the aqueous solution and obtained precipitates were moved into a Teflon liner and hydrothermally reacted under different temperatures (T_h, 180, 200 and 220 °C) for 6 h. Finally, the powders obtained were used as the specimens after washing by deionized water and absolute ethylalcohol for several times, respectively.

2.2 Characterization

The phase identification was carried out by using an X-ray diffractometer (XRD, Rigaku D/max-2550V/PC) with Cu Kα radiation and a Fourier transformed infrared spectrometer (FTIR, Nicolet 6700). The micrographs were obtained by using a field emission scanning electron microscope (FESEM, Zeiss Merlin Compact). The magnetic hysteresis loops (MHLs) were measured on a vibrating sample magnetometer (VSM, Lakeshore 7410) under a maximum external field $H_m = 1591$ kA/m (~20,000 Oe).

3 Results and discussion

3.1 Phase composition and microstructure

In our previous experiments, it was found that Fe_2O_3 is the most common impurity in the specimens obtained via a hydrothermal process, which can be ascribed to the existence of amphoteric $Zn(OH)_2$ in the precursor of hydrothermal reaction [10]. Therefore, it is necessary to use the starting materials with low Fe content to synthesize the single-phase MnZn ferrites in this study.

Figure 1 gives the XRD patterns of MnZn ferrites synthesized with the same *DF* (6%) but different T_h. Seen from the figure, there is typical peak information from spinel structure (JCPDS no. 22-1012), which suggests the formation of spinel MnZn ferrites in the specimens. However, there are also impurity peaks from Fe_2O_3 (JCPDS no. 33-0664) in the figures. Moreover, seen from the relative intensity of peaks from Fe_2O_3, the content of Fe_2O_3 increases with the increase of temperature from 180 to 220 °C. Obviously, a higher temperature may have an adverse effect on the phase formation of MnZn ferrite during a hydrothermal process. In order to synthesize single-phase MnZn ferrite, the specimens with $DF = 7\%$ were synthesized at different T_h, and the corresponding XRD patterns are shown in Fig. 2. Compared with the standard pattern of typical spinel structure (JCPDS no. 22-1012), no impurity peak can be found in Fig. 2a, which suggests a single-phase specimen of MnZn ferrite for $T_h = 180$ °C and $DF = 7\%$. However, there are still small impurity peaks from Fe_2O_3 in the XRD patterns of specimens with

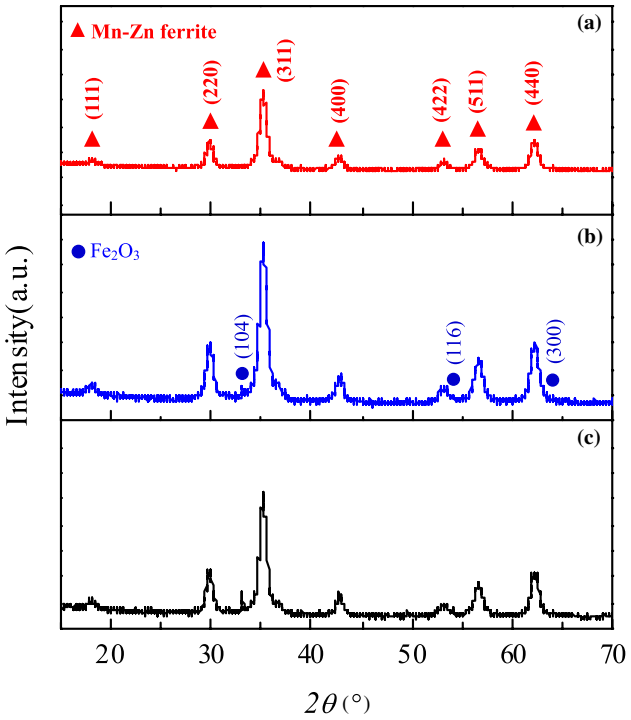

Fig. 1 XRD patterns of MnZn ferrite specimens synthesized with $DF = 6\%$. *a* $T_h = 180$ °C, *b* $T_h = 200$ °C, and *c* $T_h = 220$ °C

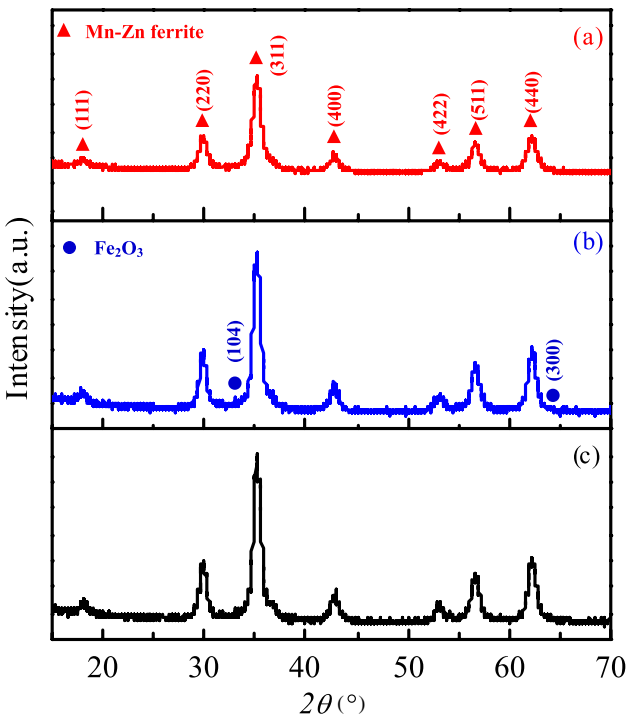

Fig. 2 XRD patterns of MnZn ferrite specimens synthesized with $DF = 7\%$. *a* $T_h = 180$ °C, *b* $T_h = 200$ °C, *c* $T_h = 220$ °C

T_h = 200 and 220 °C. Obviously, the low Fe content in starting materials and the hydrothermal temperature affect the phase formation of MnZn ferrites greatly during a hydrothermal process.

In order to confirm the formation of spinel structure, the FTIR spectra of specimens synthesized with DF = 7% were measured and given in Fig. 3. As is well-known, Fe^{3+} ion can occupy both the tetrahedral and the octahedral sites in a spinel structure. In Fig. 3, the characteristic band around 563 and 400 cm^{-1} can be attributed to the vibrations of Fe–O (Fe^{3+}) bond in the tetrahedral and octahedral sites, respectively [11, 12]. It is also found that though there is impurity Fe_2O_3 in the specimens of T_h = 200 and 220 °C, no obvious difference can be found for the FTIR spectra, suggesting a small amount of impurity in these specimens. The result of FTIR confirms the formation of MnZn ferrites further.

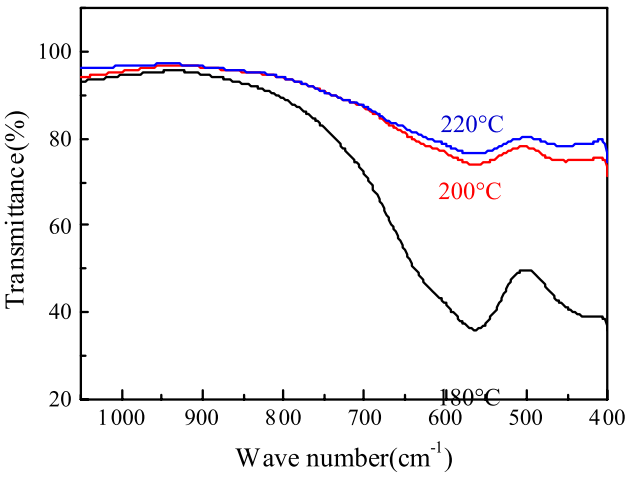

Fig. 3 FTIR spectra of MnZn ferrite specimens synthesized with DF = 7%

Figure 4 is the SEM images of MnZn ferrites synthesized with DF = 7%. It is found that all the specimens consist of ultrafine nanoparticles. Compared with some pervious reports [13, 14], our specimens exhibit a more uniform distribution of grains. Several particles' size has been marked in Fig. 4c. Compared Fig. 4c with a and b, there is a marked increasing tendency of average grain size from less than 10 nm to more than 20 nm with the increase of T_h from 180 to 220 °C. Obviously, the hydrothermal temperature has a significant effect on the topography of MnZn nanoferrites.

3.2 Magnetic properties

The magnetic hysteresis loops of MnZn ferrites synthesized with different DF and T_h measured on a VSM are shown in

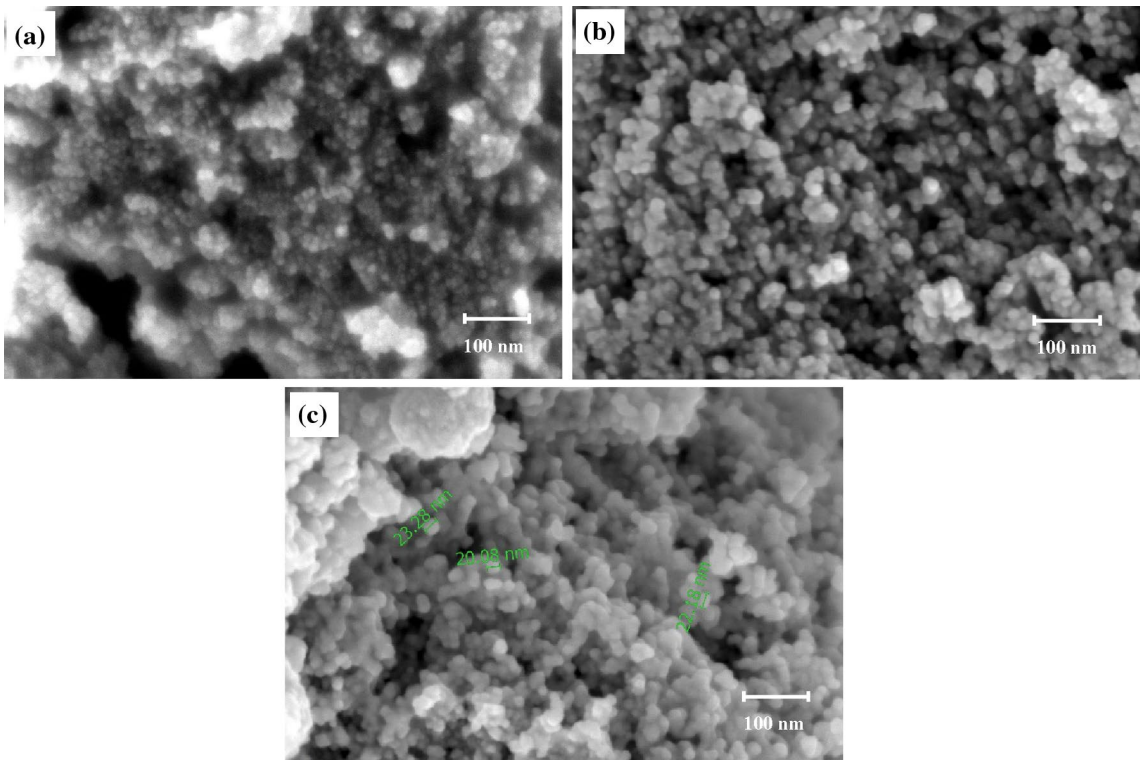

Fig. 4 SEM images of MnZn ferrite specimens synthesized with DF = 7%. T_h: **a** 180 °C, **b** 200 °C and **c** 220 °C

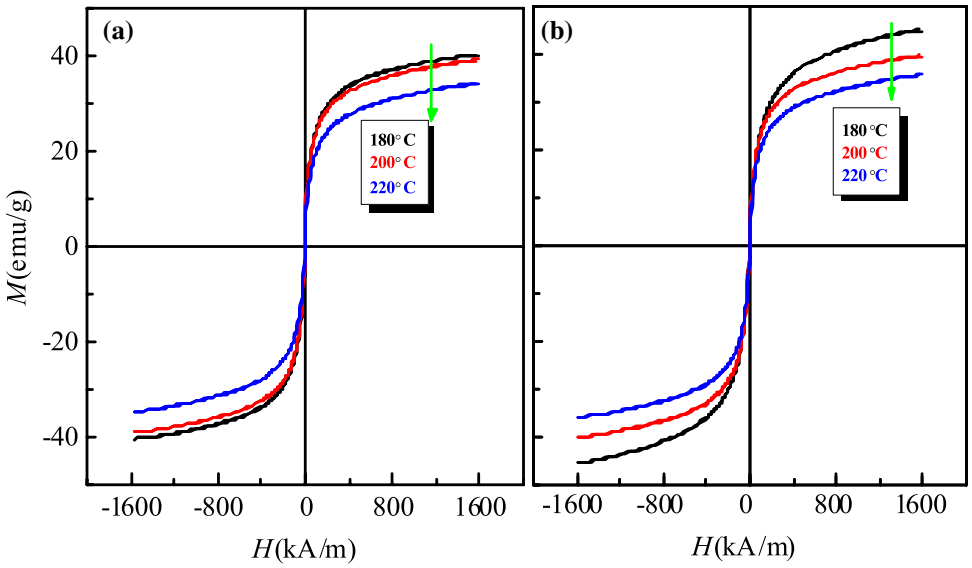

Fig. 5 Magnetic hysteresis loops of MnZn ferrite specimens synthesized with different DF and T_h. **a** $DF=6\%$ and **b** $DF=7\%$

Table 1 The main magnetic properties of MnZn nanoferrites

T_h (°C)	DF (%)	M_s (emu/g)	H_c (kA/m)
180	6	40.4	1.03
	7	45.5	0.68
200	6	39.3	0.59
	7	40.0	0.75
220	6	34.7	0.70
	7	35.9	0.62

Fig. 5, and the corresponding saturation magnetization (M_s) and coercivity (H_c) are listed in Table 1.

The H_c of most specimens is lower than 0.8 kA/m (10 Oe), exhibiting a typical and fine soft magnetic property. However, the H_c is decided not only by the intrinsic properties, such as the chemical composition and crystalline structure, but also by the extrinsic properties, such as the average crystallite size, morphology, stress, lattice defects and so on [15]. Seen from Table 1, the variation of H_c is obviously irregular.

As is known, due to the surface effect of magnetic nanoparticles [16], the M_s should decrease with the decrease of average grain size in MnZn ferrites. Seen from Fig. 4, the grain size of specimens increases obviously with the increase of T_h. However, in Table 1, it can be found a marked decreasing tendency of M_s with the increase of T_h. Combined with the results of XRD, it is clear that the effect from the impurity on M_s exceeds that from the surface effect. In addition, compared with the specimens synthesized with $DF=6\%$, the M_s of the corresponding specimens with $DF=7\%$ and the same T_h is larger, which is also can be attributed to the effect of impurity. The specimens with $DF=7\%$ have less impurity than that of the corresponding specimens with $DF=6\%$. In general, the specimen with $DF=7\%$ and $T_h=180\,°C$ whose M_s is 45.5 emu/g and H_c is 0.68 kA/m (8.6 Oe) exhibits the best soft magnetic properties.

4 Conclusions

Single-phase MnZn ferrites were successfully synthesized via a hydrothermal method using starting materials with a low Fe content. It is found that both a low Fe content and the hydrothermal temperature play crucial roles in the formation of single phase MnZn ferrite, which consequently affects the topography and the magnetic properties markedly. When $DF=7\%$ and $T_h=180\,°C$, the obtained specimen exhibits the best soft magnetic properties (M_s, 45.5 emu/g; H_c, 0.68 kA/m).

Acknowledgements This work was supported by the Provincial Training Programs of Innovation and Entrepreneurship for College Students (TPIECS) under Grant No. 201510360134.

References

1. Y.D. Peng, L.L. Chen, H.W. Ren, L.Y. Li, J.H. Yi, Q.L. Xia, J. Mater. Sci. **27**, 587 (2016)
2. H.W. Cheng, J. Li, S. Wong, C.J. Zhong, Nanoscale **8**, 19359 (2016)
3. M.J.N. Isfahani, M. Myndyk, D. Menzel, A. Feldhoff, J. Amighian, V. Šepelák, J. Magn. Magn. Mater. **321**, 152 (2009)
4. L. Lutsev, V. Shutkevich, J. Phys. D **49**, 505002 (2016)
5. S.A.S. Ebrahimi, S.M. Masoudpanah, H. Amiri, M. Yousefzadeh, Ceram. Int. **40**, 6713 (2014)
6. W.O. Choi, W.H. Kwon, K.P. Chae, Y.B. Lee, J. Magn. **21**, 40 (2016)

7. R.M. Freire, T.S. Ribeiro, I.F. Vasconcelos, J.C. Denardin, E.B. Barros, G. Mele, L. Carbone, S.E. Mazzetto, P.B.A. Fechine, J. Nanopart. Res. **15**, 1616 (2013)
8. R.M. Freire, P.G.C. Freitas, T.S. Ribeiro, I.F. Vasconcelos, J.C. Denardin, G. Mele, L. Carbone, S.E. Mazzetto, P.B.A. Fechine, Microfluid. Nanofluid. **17**, 233 (2014)
9. M. Rozman, M. Drofenik, J. Am. Ceram. Soc. **81**, 1757 (1998)
10. A.L. Xia, H.L. Zhang, Curr. Appl. Phys. **10**, 825 (2010)
11. R.H. Kadam, S.T. Alone, M.L. Mane, A.R. Biradar, S.E. Shirsath, J. Magn. Magn. Mater. **355**, 70 (2014)
12. I. Szczygieł, K. Winiarska, A. Bieńko, K. Suracka, D. Gaworska-Koniarek, J. Alloys Compd. **604**, 1 (2014)
13. L. Xiao, T. Zhou, J. Meng, Particuology **7**, 491 (2009)
14. L. Nalbandian, A. Delimitis, V.T. Zaspalis, E.A. Deliyanni, D.N. Bakoyannakis, E.N. Peleka, Microporous Mesoporous Mater. **114**, 465 (2008)
15. A.L. Xia, X.Z. Hu, D.K. Li, L. Chen, C.G. Jin, C.H. Zuo, S.B. Su, Electron Mater. Lett. **10**, 423 (2014)
16. A.L. Xia, C.H. Zuo, L.J. Zhang, C.X. Cao, Y. Deng, W. Xu, M.F. Xie, S.L. Ran, C.G. Jin, X.G. Liu, J. Phys. D: Appl. Phys. **47**, 415004 (2014)